# NJC

Accepted Manuscript


This is an *Accepted Manuscript*, which has been through the Royal Society of Chemistry peer review process and has been accepted for publication.

*Accepted Manuscripts* are published online shortly after acceptance, before technical editing, formatting and proof reading. Using this free service, authors can make their results available to the community, in citable form, before we publish the edited article. We will replace this *Accepted Manuscript* with the edited and formatted *Advance Article* as soon as it is available.

You can find more information about *Accepted Manuscripts* in the Information for Authors.

Please note that technical editing may introduce minor changes to the text and/or graphics, which may alter content. The journal's standard Terms & Conditions and the Ethical guidelines still apply. In no event shall the Royal Society of Chemistry be held responsible for any errors or omissions in this *Accepted Manuscript* or any consequences arising from the use of any information it contains.

ROYAL SOCIETY OF CHEMISTRY

www.rsc.org/njc

Journal Name

ARTICLE

# Cyanide-bridged Heterobimetallic Magnetic Complexes Based on Metalloporphyrinate and Tricyanometalate Building Blocks

Received 00th January 20xx,
Accepted 00th January 20xx

DOI: 10.1039/x0xx00000x

www.rsc.org/

Feng Gao,*[a] Guang-Zhou Zhu,[a] Liu Yang,[a] and Min-Xia Yao*[b]

Three cyanide-bridged metalloporphyrinate complexes with the formula {[(Tp*)Fe(CN)$_3$]$_2$[Mn(TPP)]}[Mn(TPP)(MeOH)$_2$] (**1**), {[(Tp)Cr(CN)$_3$]$_2$[Mn(TPP)]}[Mn(TPP)(MeOH)$_2$] (**2**), and {[(Tp*)Fe(CN)$_3$][Mn(TPyP)]}$_n$ (**3**) (Tp$^{*-}$ = hydrotris(3,5-dimethylpyrazol-1-yl)borate, Tp$^-$ = tris(pyrazolyl)hydroborate, TPP$^{2-}$ = tetra(phenyl)porphyrinate, and TPyP$^{2-}$ = tetra(4-pyridyl)porphyrinate) have been first synthesized based on tricyanometalate building blocks and metalloporphyrinate precursors. The crystal structures show that complexes **1** and **2** possess similar sandwich-like molecular structures composed of an anionic trimer and a cationic monomer. More interestingly, the introduction of manganese tetra(4-pyridyl)porphyrinate precursor results into the formation of an unprecedented neutral one-dimensional zigzag single chain complex **3**. Variable temperature dc magnetic measurements reveal the ferromagnetic and antiferromagnetic interaction between Mn$^{III}$ and Fe$^{III}$ centers for complexes **1** and **3**, respectively, and antiferromagnetic coupling between Cr$^{III}$ and Mn$^{III}$ centers for complex **2**. While ac magnetic susceptibility measurements mainifest only complex **3** shows the slow magnetic relaxation behavior of single-molecule magnet.

## Introduction

The interest in cyanide-bridged molecule-based magnetic materials with reduced dimensionality, such as single-molecule magnets (SMMs) and single-chain magnets (SCMs), has increased exponentially during the past two decades, owing to their fascinating molecular architectures and promising applications in magnetic storage, sensors, and nanoscale electronic devices.[1–4]

So far, many cyanide-bridged transition metal SMMs or SCMs have been reported.[1,2,5,6] To obtain such low-dimensional cyanide-containing magnetic complexes, one of the synthetic strategies is to utilize modified cyanometalates as building blocks toward coordinatively unsaturated metal precursors containing various ancillary ligands, in which magnetic coupling interaction between neighbouring paramagnetic metal centers can be easily controlled and anticipated.

It is worth noting that the selection of suitable ancillary functional ligands to construct the metal coordination precursors is the most effective method for rationally designing and synthesizing unusual cyanide-bridged molecular magnetic materials.[5c,7] As a representative, the macrocyclic porphyrin and its derivatives, which have been intensively studied in the field of catalysis, magnetism, nonlinear optics and sensors, can provide a tunable platform to present multidentate coordination sites along with tailored functionality at the molecular periphery for assembly-directing various metal ions.[7b,8,9] Furthermore, the introduction of such a highly conjugated and functionalized metalloporphyrinate precursor into the SMMs or SCMs will extend the research of the multifunctional molecular magnetic materials due to their intriguing structures and unique chemical/physical properties.

Herein, as a part of our continual efforts to develop new low-dimensional coordination compounds, three cyanide-bridged metalloporphyrinate complexes with the formula {[(Tp*)Fe(CN)$_3$]$_2$[Mn(TPP)]}[Mn(TPP)(MeOH)$_2$] (**1**), {[(Tp)Cr(CN)$_3$]$_2$[Mn(TPP)]}[Mn(TPP)(MeOH)$_2$] (**2**), and {[(Tp*)Fe(CN)$_3$][Mn(TPyP)]}$_n$ (**3**) (Tp$^{*-}$ = hydrotris(3,5-dimethylpyrazol-1-yl)borate, Tp$^-$ = tris(pyrazolyl)hydroborate, TPP$^{2-}$ = tetra(phenyl)porphyrinate, and TPyP$^{2-}$ = tetra(4-pyridyl)porphyrinate) have been first synthesized by the reaction of various tricyanometalate building blocks and metalloporphyrinate precursors (Scheme 1). These complexes were structurally characterized and their spectroscopic, and magnetic properties were also studied. To the best of our knowledge, cyanide-bridged transition metal complexes based on metalloporphyrinate are still scarce,[10] and there are no reports about such cationic-anionic polynuclear or neutral one-dimensional (1D) cyanide-bridged metalloporphyrinate magnetic complexes mainly based on tricyanometalate building blocks. The meaningful structure-property

[a] School of Chemistry and Chemical Engineering, Jiangsu Key Laboratory of Green Synthetic Chemistry for Functional Materials, Jiangsu Normal University, Xuzhou 221116, P. R. China.
E-mail: gaofeng_xz2002@163.com
[b] School of Chemistry and Molecular Engineering, Nanjing Tech University, Nanjing 211816, P. R. China.
E-mail:yaomx@njtech.edu.cn

† Electronic Supplementary Information (ESI) available: CCDC 1417664 (**1**), 1417665 (**2**), and 1417666 (**3**); the supplementary tables, figures, additional characterization data and X-ray crystallographic files in CIF format for all the compounds. See DOI: 10.1039/x0xx00000x

relationship obtained will improve our understanding of the magnetic behaviours of novel cyanide-bridged molecular magnetic materials.

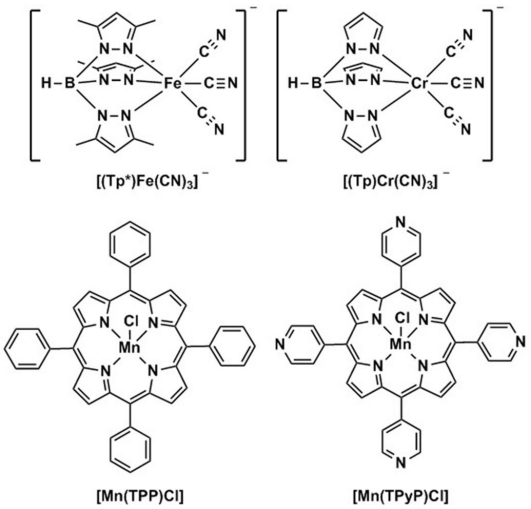


**Scheme 1** Structures of tricyanometalate building blocks (top) and metalloporphyrinate compounds (bottom).

## Experimental section

### General methods

All reagents and solvents were purchased from commercial suppliers and used without further purification. (n-$Bu_4N$)[(Tp*)$Fe(CN)_3$][11], (n-$Bu_4N$)[(Tp)$Cr(CN)_3$][12], [Mn(TPP)Cl][13], and [Mn(TPyP)Cl][14] were synthesized according to literature procedures, respectively. Elemental analyses were carried out with an Elementar Vario MICRO analyzer. IR spectra were recorded on a Vector22 Bruker spectrophotometer with KBr pellets. UV-Vis spectra were obtained with a UV−3600 spectrophotometer. Magnetic susceptibility measurements for polycrystalline samples were performed using a Quantum Design MPMS-SQUID-VSM magnetometer. Direct current (dc) magnetic susceptibility data measurements were collected between 1.8 and 300 K for dc applied fields ranging from 0 to 70 kOe. Alternating-current (ac) magnetic susceptibility data measurements were carried out under an oscillating field of 2 Oe and ac frequencies ranging between 1 and 997 Hz. Diamagnetic corrections were applied for the sample holder and calculated using Pascal's constants.[15]

### X-ray Crystallography

All of the crystal structures were determined at 296(2) K on a Bruker APEX CCD diffractometer using monochromated Mo Kα radiation (λ = 0.71073 Å). Diffraction data analysis and reduction were performed within *SMART* and *SAINT*.[16] Absorption corrections were applied by *SADABS* program.[17] The crystal structures were solved by direct methods and refined by full-matrix least-squares based on $F^2$ using the *SHELXTL* program[18] with anisotropic displacement parameters for all non-hydrogen atoms. Hydrogen atom positions were calculated geometrically and were riding on their respective atoms. The remaining solvent molecules were removed by the SQUEEZE routine in PLATON.[19] More details for the data collections and structure refinements are given in Table 1. The selected bond lengths and bond angles were listed in Tables S1−S3†. (CCDC no. 1417664 (**1**), 1417665 (**2**), and 1417666 (**3**)).

**Synthesis of {[(Tp*)Fe(CN)$_3$]$_2$[Mn(TPP)]}[Mn(TPP)(MeOH)$_2$] (1).** The reaction mixture of [MnTPPCl] (17.58 mg, 0.025 mmol) and (n-$Bu_4N$)[(Tp*)$Fe(CN)_3$] (16.84 mg, 0.025 mmol) in 10 mL of methanol/acetone (1:1 v/v) was stirred at room temperature for 12 h. Brown block-shaped crystals of **1** were obtained after slow evaporation of the filtrate for several days. Yield: 65%. Anal. Calcd for $C_{126}H_{108}B_2Fe_2Mn_2N_{26}O_2$: C 66.92; H 4.81; N 16.10. Found: C 67.11; H 5.09; N 16.36. Selected IR data (KBr, $cm^{-1}$): 3402(w), 2920(m), 2524(m), 2127(s), 1636(s), 1486(s), 1201(s), 1009(s), 799(m), 753(m), and 702(m). Selected UV-Vis data ($CH_2Cl_2$, $\lambda_{max}$/nm): 341, 390, 481, 579, and 617.

**Synthesis of {[(Tp)Cr(CN)$_3$]$_2$[Mn(TPP)]}[Mn(TPP)(MeOH)$_2$] (2).** The brown block-shaped crystals of complex **2** were obtained by following the same procedure for complex **1** but using (n-$Bu_4N$)[(Tp)$Cr(CN)_3$] instead of (n-$Bu_4N$)[(Tp*)$Fe(CN)_3$]. Yield: 65%. Anal. Calcd for $C_{114}H_{76}B_2Cr_2Mn_2N_{26}O_2$: C 65.91; H 3.69; N 17.53. Found: C 66.19; H 3.85; N 17.84. Selected IR data (KBr, $cm^{-1}$): 3411(w), 2917(m), 2492(m), 2132(s), 1628(s), 1495(m), 1308(s), 1206(m), 1029(m), 1010(s), 815(m), 757(m), and 707(m). Selected UV-Vis data ($CH_2Cl_2$, $\lambda_{max}$/nm):339, 392, 479, 580, and 617.

**Synthesis of {[(Tp*)Fe(CN)$_3$][Mn(TPyP)]}$_n$ (3).** The brown block-shaped crystals of complex **3** were obtained by following the same procedure for complex **1** but using [MnTPyPCl] instead of [MnTPPCl]. Yield: 45%. Anal. Calcd for $C_{58}H_{46}BFeMnN_{17}$: C 63.17; H 4.20; N 21.59. Found: C 63.50; H 4.39; N 21.85. Selected IR data (KBr, $cm^{-1}$): 3397(w), 2932(m), 2531(m), 2128(s), 1640(s), 1599(m), 1425(m), 1311(s), 1225(m), 1116(s), 1011(m), 799(m), 732(m), and 687(m). Selected UV-Vis data ($CH_2Cl_2$, $\lambda_{max}$/nm): 342, 373, 399, 476, 576, and 611.

## Results and discussion

### Synthesis and characterization

All the complexes were successfully synthesized based on tricyanometalate building blocks and various metalloporphyrinate precursors. By equivalent molar reaction of five-coordinated [Mn(TPP)Cl] with $[(Tp^*)Fe(CN)_3]^-$ or $[(Tp)Cr(CN)_3]^-$ can obtain two sandwich-type trinuclear cyanide-bridged anionic complexes $[Fe^{III}\text{-}Mn^{III}\text{-}Fe^{III}]^-$ (**1**), or $[Cr^{III}\text{-}Mn^{III}\text{-}Cr^{III}]^-$ (**2**), respectively, with a larger balance cation $[Mn(TPP)(MeOH)_2]^+$. However, the reaction of $[(Tp^*)Fe(CN)_3]^-$ with manganese(III) tetra(4-pyridyl)porphyrinate precursor [Mn(TPyP)Cl] containing electron-donating pyridyl substituents results into the formation of a neutral 1D zigzag single chain complex **3**. These compounds have been characterized by

Journal Name

ARTICLE

**Table 1** Crystallographic data for complexes **1**–**3**.

| | **1** | **2** | **3** |
|---|---|---|---|
| formula | $C_{126}H_{108}B_2Fe_2Mn_2N_{26}O_2$ | $C_{114}H_{82.55}B_2Cr_2Mn_2N_{26}O_{2.28}$ | $C_{58}H_{46}BFeMnN_{17}$ |
| fw | 2261.58 | 2088.50 | 1102.72 |
| crystal system | Triclinic | Monoclinic | Monoclinic |
| space group | Pī | P2(1)/c | P2(1)/c |
| *a* / Å | 13.471(3) | 19.758(3) | 20.928(7) |
| *b* / Å | 14.060(3) | 12.4162(17) | 14.437(4) |
| *c* / Å | 18.498(4) | 22.828(3) | 20.777(6) |
| *α* / deg | 106.035(3) | 90 | 90 |
| *β* / deg | 103.800(3) | 105.308(2) | 105.019(3) |
| *γ* / deg | 92.507(3) | 90 | 90 |
| *V* / Å$^3$ | 3247.3(10) | 5401.5(13) | 6063(3) |
| *Z* | 1 | 2 | 4 |
| $\rho_{calcd}$, g cm$^{-3}$ | 1.156 | 1.284 | 1.208 |
| *T* / K | 296(2) | 296(2) | 296(2) |
| *μ* / mm$^{-1}$ | 0.466 | 0.487 | 0.498 |
| *ϑ* / deg | 1.19–25.50 | 1.85–25.51 | 1.73–25.51 |
| *F*(000) | 1174 | 2149 | 2276 |
| data / parameters | 11956 / 768 | 10006 / 662 | 11155 / 709 |
| GOF ($F^2$) | 1.104 | 1.066 | 1.021 |
| $R_1$, $wR_2$ (I>2σ(I)) | 0.0575, 0.1879 | 0.0623, 0.1737 | 0.1146, 0.2569 |
| $R_1$, $wR_2$ (all data) | 0.0727, 0.2004 | 0.0762, 0.1843 | 0.1345, 0.2674 |

elemental analysis, IR, UV-Vis, and suitable single crystals for X-ray diffraction analysis were obtained by slow evaporation of the solution of these complexes in methanol and acetone. The electronic absorption spectra of metalloporphyrinate precursors and the targeted complexes in $CH_2Cl_2$ solution are almost identical with high intensity Soret bands around 480 nm and weaker Q–bands above 575 nm (Figure S1†), which can be assigned to the intra-ligand π–π* transitions of the porphyrin and its derivatives.[13]

**Crystal structures of complexes 1 and 2**

The crystal structures of complexes **1** and **2** are similar, crystallizing in the triclinic (**1**) and monoclinic (**2**) system with space group Pī and P2(1)/c, respectively. Both of them possess a similar sandwich-like molecular structure made up of an anionic trinuclear entity $[(Tp^*)Fe(CN)_3]_2[Mn(TPP)]^-$ (**1**) or $[(Tp)Cr(CN)_3]_2[Mn(TPP)]^-$ (**2**) with the free $[Mn(TPP)(MeOH)_2]^+$ as a balance cation, respectively. In the anionic trinuclear unit, the tricyanometalate building block acts as a monodentate linker through one of its three cyanide groups towards the central $Mn^{III}$ ion from $Mn(TPP)^+$ fragment. The central Fe(1) or Cr(1) ion situates in a slightly distorted octahedral coordination environment, bonded by three N (pyrazolyl groups) atoms and three C (cyanide groups) atoms with average Fe–N(pyrazolyl) bond length of 2.003 Å for **1**, and Cr–N(pyrazolyl) bond length of 2.052 Å for **2**, while Mn(1) ion is coordinated by six N atoms (four from porphyrinate ligand located in a perfect equatorial plane and two axial position from the bridging cyanide groups) (Figures 1 and 2). In addition, the distance of Mn(1)–N(pyrrolyl) is shorter than the Mn(1)–N(cyanide) bond length, and the corresponding Mn(1)–N≡C bond angle deviates significantly from linearity, indicating the obviously distorted octahedron surrounding the Mn(1) ion. In countercationic segment $[Mn(TPP)(MeOH)_2]^+$, the central metal ion is also six-coordinated by four pyrrolyl nitrogen atoms of the porphyrinate ligand and two oxygen atoms from neutral methanol molecules. It should be noted that the highly distorted structure and the size of metalloporphyrinate precursor may hinder the formation of one-dimensional (1D) chain structure. The intramolecular cyanide-bridged

Fe(1)···Mn(1) distance for **1** is 5.263(5) Å, and Cr(1)···Mn(1) distance for **2** is 5.432(6) Å, while the shortest intermolecular metal-metal separation among anionic trinuclear units is 13.471(4) (Mn···Mn), 8.153(3) (Fe···Fe), and 10.217(3) Å (Fe···Mn) for **1**, and 12.416(3) (Mn···Mn), 8.320(4) (Cr···Cr), and 9.065(3) Å (Cr···Mn) for **2**, respectively. Additionally, the intermolecular hydrogen-bond interactions can be found for complex **2** between the nitrogen atom of the cyanide group and the oxygen atom of the uncoordinated $[Mn(TPP)(MeOH)_2]^+$ (Figures S2 and S3†).

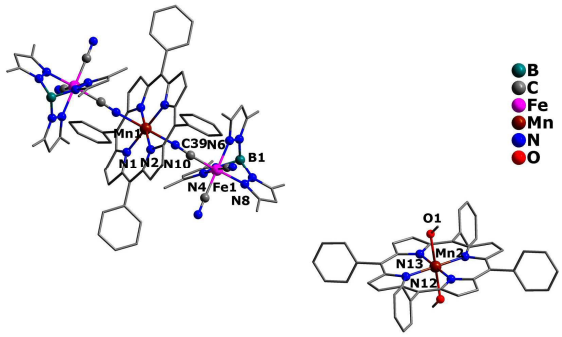


**Fig. 1** Crystal structure of complex **1** with hydrogen atoms omitted for clarity.

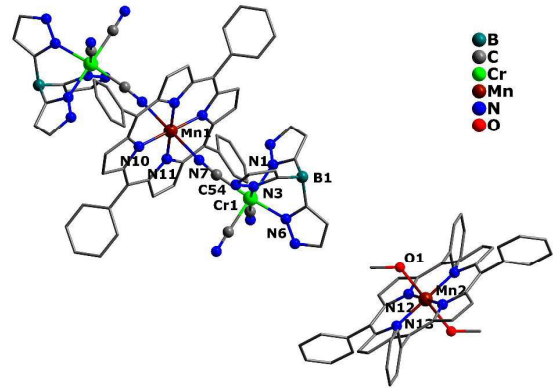


**Fig. 2** Crystal structure of complex **2** with hydrogen atoms and solvent molecules omitted for clarity.

### Crystal structure of complex 3

Unlike above mentioned two cationic-anionic polynuclear complexes, complex **3** has been structurally characterized as neutral 1D zigzag single chain crystallizing in monoclinic system P2(1)/c space group. As shown in the Figure 3, each $[(Tp^*)Fe(CN)_3]^-$ entity acts as a monodentate ligand toward the $[Mn(TPyP)]^+$ unit through one of its three cyanide groups, whereas $Mn^{III}$ tetra(4-pyridyl)porphyrinate precursor is linked to each other by one pyridyl N atom coming from the tetra(4-pyridyl)porphyrinate ligand. The coordination geometries around both $Fe^{III}$ and $Mn^{III}$ ions are all octahedral, in which $Fe^{III}$ ion is bonded by three pyrazolyl N atoms and three cyanide C atoms, while $Mn^{III}$ ion is occupied by equatorial N4 donor atoms from porphyrinate ligand, one apical N atom from pyridyl group, and one cyanide N atom. The average Fe–N(pyrazolyl) and Mn–N bond lengths are 1.988 and 2.104 Å, respectively, and the shortest intrachain Fe···Mn, Mn···Mn and Fe···Mn distances are 5.238(4), 10.093(3), and 14.437(4) Å. However, in crystal packing (Figure S4†), the shortest interchain metal-metal separations are 10.586(4) Å for Fe···Fe, 11.494(3) Å for Mn···Mn, and 11.399(3) Å for Fe···Mn, respectively.

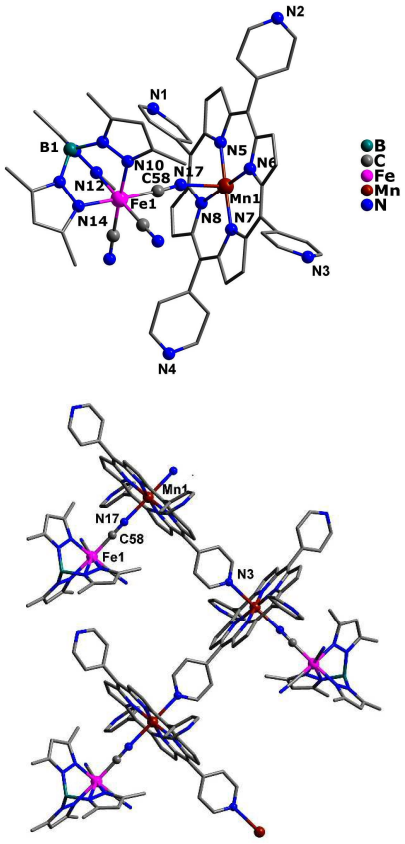


**Fig. 3** Crystal structure of complex **3** for its asymmetric unit (top) and one-dimensional zigzag infinite chain (bottom) with hydrogen atoms omitted for clarity, respectively.

### Magnetic properties

The variable-temperature dc magnetic susceptibilities for all of the complexes were measured under an applied dc field of 100 Oe in the temperature range of 1.8–300 K. For complex **1**, the $\chi_M T$ value at room temperature is 6.65 $cm^3 \cdot K \cdot mol^{-1}$ (Figure 4), which is close to the value of 6.75 $cm^3 \cdot K \cdot mol^{-1}$ expected for uncoupled two low-spin $Fe^{III}$ centers ($S$ = 1/2) and two high-spin $Mn^{III}$ centers ($S$ = 2) assuming $g$ = 2.00. Upon cooling, $\chi_M T$ value increases gradually and reaches the maximum value of 7.95 $cm^3 \cdot K \cdot mol^{-1}$ at 6.5 K, suggesting the presence of the ferromagnetic coupling between the $Fe^{III}$ and $Mn^{III}$ ions mediated by cyanide group. While the $\chi_M T$ value starts to decrease rapidly to 7.23 $cm^3 \cdot K \cdot mol^{-1}$ at 1.8 K, probably ascribed to the intermolecular antiferromagnetic coupling and/or the zero-field splitting (ZFS) of the $Mn^{III}$ ion at such low temperature region.[6i,10d,20] On the basis of the trimeric model, the magnetic susceptibilities can be fitted accordingly by the following expression derived from the isotropic exchange spin

Hamiltonian $\hat{H} = -2J\hat{S}_{Mn1}(\hat{S}_{Fe1}+\hat{S}_{Fe2})$, in which we assume equivalent interaction among the central $Mn^{III}$ ion and the two $Fe^{III}$ ions, and neglect the magnetic interaction between the terminal $Fe^{III}$ ions.[21] The free $Mn^{III}$ anion was included as a constant term ($\chi_M T = (Ng^2\beta^2/3k)S_{Mn2}(S_{Mn2}+1)$). The best fit between 1.8 and 300 K gave $g$ = 1.96, $J$ = 2.95 $cm^{-1}$ and $zj'$ = −0.025 $cm^{-1}$ ($R = 2.68 \times 10^{-3}$). Furthermore, the magnetic susceptibility above 50 K obeys the Curie–Weiss law $\chi_M = C/(T-\theta)$ with a Curie constant $C$ = 6.54 $cm^3\cdot K\cdot mol^{-1}$ and a Weiss constant $\theta$ = 2.46 K (insert of Figure 4). The C value corresponds to magnetically isolated $Fe^{III}$ and $Mn^{III}$ ions, while the positive $\theta$ also suggests dominant ferromagnetic coupling in complex **1**. The field-dependent measurement of the magnetization up to 70 kOe was also carried out for **1** at 1.8 K. The magnetization increases rapidly at low field and then slowly reaches a maximum value of 7.71 $N\beta$ (Figure S5†), which further confirm that ferromagnetic coupling interactions exist between the $Fe^{III}$ and $Mn^{III}$ ions.[10d]

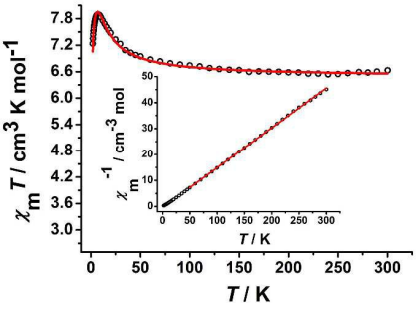


**Fig. 4** Temperature-dependent $\chi_M T$ product for **1** at 100 Oe. The red solid line represents the best fits of the data. Inset: Plots of $1/\chi_M$ versus $T$. The red solid line is the fitting result by Curie-Weiss law.

The temperature-dependent $\chi_M T$ product for complex **2** is shown in Figure 5, the $\chi_M T$ value at 300 K is 8.97 $cm^3\cdot K\cdot mol^{-1}$, which is basically consistent with the value of 9.75 $cm^3\cdot K\cdot mol^{-1}$ for uncoupled two high-spin $Mn^{III}$ centers ($S$ = 2) and two $Cr^{III}$ centers ($S$ = 3/2) based on $g$ = 2.00. With decreasing the temperature, the $\chi_M T$ value decreases gradually and then rapidly reaches the lowest value of 5.13 $cm^3\cdot K\cdot mol^{-1}$ at 1.8 K. This behaviour may be caused by the antiferromagnetic coupling between the $Cr^{III}$ and $Mn^{III}$ ions and/or the ZFS effect of the $Mn^{III}$ ion.[10a] On the basis of the trimeric model, the magnetic susceptibilities can be fitted accordingly by the following expression derived from the isotropic exchange spin Hamiltonian $\hat{H} = -2J\hat{S}_{Mn1}(\hat{S}_{Cr1}+\hat{S}_{Cr2})$, which includes only nearest-neighbour exchange and the interaction among the central $Mn^{III}$ ion and the two $Cr^{III}$ ions is equivalent.[21] The free $Mn^{III}$ anion was included as a constant term ($\chi_M T = (Ng^2\beta^2/3k)S_{Mn2}(S_{Mn2}+1)$). The best fit between 14 and 300 K gave $g$ = 1.91 and $J$ = −0.63 $cm^{-1}$ ($R = 7.32 \times 10^{-3}$). The magnetic susceptibilities conform well to Curie–Weiss law above 50 K, giving a Curie constant $C$ = 9.11 $cm^3\cdot K\cdot mol^{-1}$ and a Weiss constant $\theta$ = −5.95 K (insert of Figure 5). The negative $\theta$ also confirms the antiferromagnetic coupling in complex **2**. The field dependence of the magnetization of complex **2** measured at 1.8 K (Figure S6†) with the value of 10.18 $N\beta$ *at* 70 kOe is obviously lower than the value of uncoupled two $Mn^{III}$ (S = 2) and two $Cr^{III}$ (S = 3/2) based on g = 2.0, confirming the antiferromagnetic coupling interaction between $Cr^{III}$ and $Mn^{III}$ ions bridged by cyanide group.[10e]

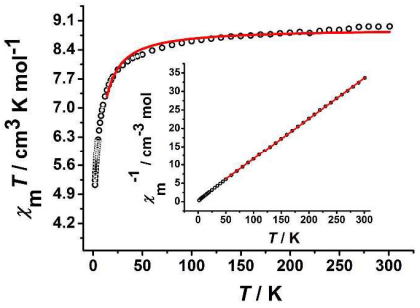


**Fig. 5** Temperature-dependent $\chi_M T$ product for **2** at 100 Oe. The red solid line represents the best fits of the data. Inset: Plots of $1/\chi_M$ versus $T$. The red solid line is the fitting result by Curie-Weiss law.

For neutral 1D single chain complex **3**, the room-temperature $\chi_M T$ value is 3.35 $cm^3\cdot K\cdot mol^{-1}$ (Figure 6), close to the value of 3.38 $cm^3\cdot K\cdot mol^{-1}$ expected for a low-spin $Fe^{III}$ center ($S$ = 1/2) and a high-spin $Mn^{III}$ center ($S$ = 2) assuming $g$ = 2.00 and no exchange coupling. Between 300 and 60 K, $\chi_M T$ product gradually decreases and reaches a minimum value of 3.20 at 60 K. While the $\chi_M T$ product increases to a maximum value of 3.24 $cm^3\cdot K\cdot mol^{-1}$ at 16 K and then decreases further to 2.82 $cm^3\cdot K\cdot mol^{-1}$ at 1.8 K, suggesting that the presence of antiferromagnetic coupling between $Fe^{III}$ and $Mn^{III}$ centers with the cooperation of ZFS of $Mn^{III}$ ion.[6i] Due to the long Mn···Mn distance of 10.093(3) Å within the chain, the intrachain magnetic interactions between $Mn^{III}$ and $Mn^{III}$ ions is very weak and can be negligible. Only the magnetic couplings between neighbouring $Fe^{III}$ and $Mn^{III}$ ions through cyanide bridges are considered. In order to evaluate the strength of intra-/inter-dimer magnetic coupling (J/zJ') and zfs parameter (D) of Mn(III), the best fit for the experimental magnetic data above 60 K based on the equation[6i]:

$$\hat{H} = -2J\hat{S}_{Mn}\cdot\hat{S}_{Fe} + D(\hat{S}_z^2 - \frac{S_{Mn}(S_{Mn}+1)}{3}) + g\beta\hat{H}S - zJ'\langle S_z^T\rangle\hat{S}_z^T$$

Affording the corresponding parameters of $g$ = 2.00, $J$ = −1.01 $cm^{-1}$ , $D$ = −1.34 $cm^{-1}$ and $zj'$ = −0.01 $cm^{-1}$ ($R = 1.6 \times 10^{-4}$). It should be mentioned that based on the powder magnetic susceptibility data it is difficult to determine the sign of $D_{Mn}$. The calculated $D_{Mn}$ value (−1.34 $cm^{-1}$) is normal for high-spin tetragonally elongated octahedral Mn(III).[6j] While the Curie constant $C$ = 3.40 $cm^3\cdot K\cdot mol^{-1}$ and the Weiss constant $\theta$ = −4.81 K can be obtained by fitting the magnetic susceptibilities above 50 K using Curie–Weiss law (insert of Figure 6). The negative $\theta$ indicating the presence of antiferromagnetic coupling in complex **3**. The curve of the field-dependent magnetization for complex **3** at 1.8 K attains a maximum value of 3.53 $N\beta$ at 70 kOe (Figure S7†), which is obviously lower than the value of uncoupled $Fe^{III}Mn^{III}$ unit based on g = 2.0, confirming again the existence of antiferromagnetic coupling interaction between the neighbouring $Fe^{III}$ and $Mn^{III}$ ions and/or the ZFS effect of the $Mn^{III}$ ion.[6i]

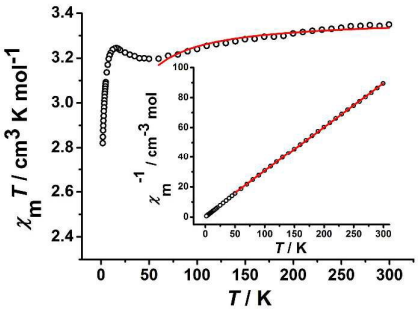


**Fig. 6** Temperature-dependent $\chi_M T$ product for **3** at 100 Oe. The red solid line represents the best fits of the data. Inset: Plots of $1/\chi_M$ versus $T$. The red solid line is the fitting result by Curie-Weiss law.

To investigate the magnetization dynamics, ac magnetic susceptibility measurements were performed on all the complexes at zero dc field. For complexes **1** and **2**, neither peaks nor obvious temperature-dependent in-phase ($\chi'$) and out-of-phase ($\chi''$) signals were observed in the frequency of 997 Hz and at temperatures down to 1.9 K (Figures S8 and S9†). While $\chi''$ component of the ac susceptibility for complex **3** increases with lowering temperature, suggesting the presence of slow relaxation effects. Unfortunately, the maxima on the $\chi''$ *vs.* $T$ curves cannot be found down to 1.9 K, even at 997 Hz (Figure S10†). Applying a static dc field of 2000 Oe, the clear peaks of $\chi''$ signal can be easily found at frequencies higher than 444 Hz (Figure 7, top), indicating the presence of thermally activated relaxation processes under such an external applied magnetic field. Fitting the data to Arrhenius law [$\tau = \tau_0 \exp(\Delta/k_B T)$] affords anisotropic energy barrier $\Delta/k_B$ = 11.73 K and pre-exponential factor $\tau_0 = 6.3 \times 10^{-7}$ s (R = 0.998) (Figure 7, bottom), which are consistent with the expected $\tau_0$ of $10^{-6}$–$10^{-11}$ s for typical SMMs.[22]

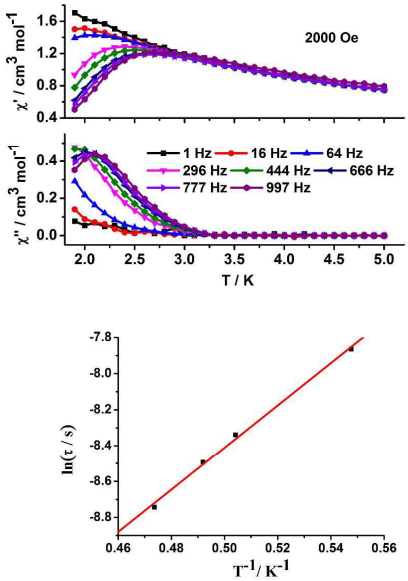


**Fig. 7** Temperature-dependent in-phase ($\chi'$) and out-of-phase ($\chi''$) ac susceptibilities for complex **3** under 2000 oe dc field at 1–997 Hz. The solid lines are guides only (top) and $\ln\tau$ versus $T^{-1}$ plots for complex **3**. Red line represents the best fit to the Arrhenius law (bottom).

**Magneto-structural correlation.**

It has been experimentally shown that the magnetic coupling between low-spin $Fe^{III}$ and high-spin $Mn^{III}$ is ferromagnetic arising from the strict orthogonality of the magnetic orbitals ($t_{2g}$ in $Fe^{III}$ *vs.* $d_z^2$ in $Mn^{III}$) or antiferromagnetic arising from the orbital overlap between them.[6i,23] The overall magnetic property depends on which contribution is predominant. Some important structural parameters, such as the Mn–N(axial) lengths and Mn–N≡C angles, affect the magnetic exchange coupling. The analysis shows the bending of the Mn–N≡C–Fe linkages and the rotation of the x and z axes for $Mn^{III}$ can enlarge the overlap and therefore weaken the ferromagnetic contribution. In our paper, the length of Mn–N(equatorial) is shorter than the Mn–N(axial), and the Mn–N≡C bond angle (168.8(3)° for **1** and 164.4(7)° for **3**) deviates significantly from linearity, indicating the obviously distorted octahedron surrounding the central Mn ion, associated with the ferromagnetic and antiferromagnetic interaction between neighbouring $Mn^{III}$ and $Fe^{III}$ ions for complexes **1** and **3**, respectively. By investigating some similar cyanide-bridged heterobimetallic $Fe^{III}$–$Mn^{III}$ complexes reported previously,[6i,10d,10f,23,24] it can be also found that the ferromagnetic interactions become weak while the antiferromagnetic interactions become strong with the bending of the Mn–N≡C angles. However, the antiferromagnetic coupling interaction can usually be investigated through the orbital overlap between $t_{2g}$ orbitals of $Cr^{III}$ and $Mn^{III}$ for the cyanide-bridged $Cr^{III}$–$Mn^{III}$ complexes,[25] similar to complex **3** as we reported.

## Conclusions

Three cyanide-bridged heterobimetallic complexes have been synthesized based on tricyanometalate building blocks and various metalloporphyrinate precursors. Complexes **1** and **2** show similar molecular structures composed of an anionic trimer and a cationic monomer. However, the introduction of manganese(III) tetra(4-pyridyl)porphyrinate precursor results into the formation of an unprecedented neutral one-dimensional zigzag single chain complex **3**. Variable temperature direct current magnetic measurements reveal the ferromagnetic and antiferromagnetic interaction between $Mn^{III}$ and $Fe^{III}$ centers for complexes **1** and **3**, respectively, and antiferromagnetic coupling between $Cr^{III}$ and $Mn^{III}$ centers for complex **2**. While dynamic magnetic properties confirm that only complex **3** exhibits the slow magnetic relaxation behavior of single-molecule magnet. More works focusing on designing and synthesizing novel cyanide-bridged magnetic complexes including such highly conjugated and functionalized metallomacrocyclic precursor with intriguing structures and unique chemical/physical properties are underway in our laboratory.

## Acknowledgements

This work was supported by the National Natural Science Foundation of China (no. 21401085 and 21401101), the Natural Science Foundation of Jiangsu Province (BK20140935),

PAPD of Jiangsu Higher Education Institutions, and the Natural Science Foundation of Jiangsu Normal University (14XLR031).

## Notes and references

1 (a) L. M. C. Beltran and J. R. Long, *Acc. Chem. Res*., 2005, **38**, 325−334; (b) M. Ohba and H. Okawa, *Coord. Chem. Rev.*, 2000, **198**, 313−328; (c) M. Atanasov, P. Comba, S. Hausberg and B. Martin, *Coord. Chem. Rev.*, 2009, **253**, 2306−2314; (d) H.-L. Sun, Z.-M. Wang and S. Gao, *Coord. Chem. Rev.*, 2010, **254**, 1081−1100; (e) R. Lescouezec, L. M. Toma, J. Vaissermann, M. Verdaguer, F. S. Delgado, C. Ruiz-Pérez, F. Lloret and M. Julve, *Coord. Chem. Rev.*, 2005, **249**, 2691−2729.

2 (a) J. H. Lim, J. H. Yoon, H. C. Kim and C. S. Hong, *Angew. Chem. Int. Ed.*, 2006, **45**, 7424−7426; (b) C.-F. Wang, J.-L. Zuo, B. M. Bartlett, S. You, J. R. Long and X.-Z. You, *J. Am. Chem. Soc.*, 2006, **128**, 7162−7163; (c) S. Wang, J.-L. Zuo, H.-C. Zhou, H. J. Choi, Y. Ke, J. R. Long and X.-Z. You, *Angew. Chem. Int. Ed.*, 2004, **43**, 5940−5943.

3 (a) S. Gatteschi and R. Sessoli, *Angew. Chem. Int. Ed.*, 2003, **42**, 268−297; (b) J. T. Culp, J.-H. Park, F. Frye, Y.-D. Huh, M. W. Meisel and D. R. Talham, *Coord. Chem. Rev.*, 2005, **249**, 2642−2648.

4 (a) R. Sessoli, D. Gatteschi, A. Caneschi and M. A. Novak, *Nature*, 1993, **365**, 141−143; (b) M. N. Leuenberger and D. Loss, *Nature*, 2001, **410**, 789−793; (c) L. Bogani and W. Wernsdorfer, *Nature Mater.*, 2008, **7**, 179–186; (d) D. A. Garanin and E. M. Chudnovsky, *Phys. Rev. B,* 1997, **56**, 11102−11118.

5 (a) S. Wang, X.-H. Ding, Y.-H. Li and W. Huang, *Coord. Chem. Rev.*, 2012, **256**, 439−464; (b) S. Wang, X.-H. Ding, J.-L. Zuo, X.-Z. You and W. Huang, *Coord. Chem. Rev.*, 2011, **255**, 1713−1732; (c) K. S. Pedersen, J. Bendix and R. Clérac, *Chem. Commun.*, 2014, **50**, 4396−4415; (d) L. Cui, F. Zhu, C. F. Leong, J. Ru, F. Gao, D. M. D'Alessandro and J. Zuo, *Sci China Chem.*, 2015, **58**, 650–657; (e) E. Gungor, Y. Yahsi, H. Kara and A. Caneschi, *CrystEngComm*, 2015, **17**, 3082–3088; (f) Y.-Z. Zhang, P. Ferko, D. Siretanu, R. Ababei, N. P. Rath, M. J. Shaw, R. Clérac, C. Mathonière and S. M. Holmes, *J. Am. Chem. Soc.*, 2014, **136**, 16854−16864; (g) D.-Y. Wu and O. Sato, *Z. Anorg. Allg. Chem.*, 2009, **635**, 389–392; (h) T. Delgado, A. Tissot, C. Desnard, L. Guénée, P. Pattison and A. Hauser, *Chem. –Eur. J.*, 2015, **21**, 3664–3670; (i) X.-J. Xu, R.-R. Zhou, J. Wang, L. Li and J.-Q. Tao, *Z. Anorg. Allg. Chem.*, 2015, **641**, 490–494.

6 (a) D. Pinkowicz, H. Southerland, X.-Y. Wang and K. R. Dunbar, *J. Am. Chem. Soc.*, 2014, **136**, 9922−9924; (b) Y.-Y. Chem, A.-Y. Hu, M.-Q. Shen, X.-Y. Tian and H. Zhou, *Z. Anorg. Allg. Chem.*, 2014, **640**, 2287–2291; (c) P.-F. Zhuang, Y.-J. Zhang, H. Zheng, C.-Q. Jiao, L. Zhao, J.-L. Wang, C. He, C.-Y. Duan and T. Liu, *Dalton Trans.*, 2015, **44**, 3393−3398; (d) J. J. Sokol, A. G. Hee and J. R. Long, *J. Am. Chem. Soc.*, 2002, **124**, 7656–7657; (e) M.-X. Yao, Q. Zheng, X.-M. Cai, Y.-Z. Li, Y. Song and J.-L. Zuo, *Inorg. Chem.,* 2012, **51**, 2140−2149; (f) M.-X. Yao, Z.-Y. Wei, Z.-G. Gu, Q. Z, Y. X. and J.-L. Zuo, *Inorg. Chem.,* 2011, **50**, 8636−8644; (g) D. Zhang, S. Zhuo, P. Wang, X. Chen and J. Jiang, *New J. Chem.*, 2014, **38**, 5470−5479; (h) H. Zhou, Y. Wang, F. Mou, X. Shen and Y. Liu, *New J. Chem.*, 2014, **38**, 5925−5934; (i) Z.-H. Ni, J. Tao, W. Wernsdorfer, A.-L. Cui and H.-Z. Kou, *Dalton Trans.*, 2009, 2788−2794; (j) D. Visinescu, L. M. Toma, J. Cano, O. Fabelo, C. Ruiz-Pérez, A. Labrador, F. Lloret and M. Julve, *Dalton Trans.*, 2010, **39**, 5028−5038.

7 (a) E. L. Gavey and M. Pilkington, *Coord. Chem. Rev.*, 2015, **296**, 125−152; (b) G. Kumar and R. Gupta, *Chem. Soc. Rev.*, 2013, **42**, 9403−9453.

8 (a) C. M. B. Carvalho, T. J. Brocksom and K. T. de Oliveira, *Chem. Soc. Rev.*, 2013, **42**, 3302−3317; (b) J. Otsuki, *Coord. Chem. Rev.*, 2010, **254**, 2311−2341; (c) K.-J. Lin, *Angew. Chem. Int. Ed.*, 1999, **38**, 2730−2732; (d) L. Pan, S. Kelly, X. Huang and J. Li, *Chem. Commun.*, 2002, 2334−2335.

9 (a) W.-Y. Gao, M. Chrzanowski and S. Ma, *Chem. Soc. Rev.*, 2014, **43**, 5841−5866; (b) H. L. Buckley and J. Arnold, *Dalton Trans.*, 2015, **44**, 30−36.

10 (a) D. Zhang, Z. Zhao, P. Wang and Z. Ni, *CrystEngComm*, 2013, **15**, 2504–2511; (b) S. Huh, K.-T. Youm, Y. J. Park, A. J. Lough, M. Ohba and M.-J. Jun, *Bull. Korean. Chem. Soc.*, 2005, **26**, 1031–1032; (c) D. Zhang, L.-F. Zhang, Y. Chen, H. Wang, Z.-H. Ni, W. Wernsdorfer and J. Jiang, *Chem. Commun.*, 2010, **46**, 3550−3552; (d) D. Zhang, H. Wang, L. Tian, H.-Z. Kou, J. Jiang and Z.-H. Ni, *Cryst. Growth Des.*, 2009, **9**, 3989−3996; (e) D. Zhang, H. Wang, Y. Chen, Z.-H. Ni, L. Tian and J. Jiang, *Inorg. Chem. Commun.*, 2009, **12**, 698−700; (f) G.-L. Li, J. Nie, H. Chen, Z.-H. Ni, Y. Zhao and L.-F. Zhang, *Inorg. Chem. Commun.*, 2012, **19**, 66−69; (g) X. Chen, S.-Q. Wu, A.-L. Cui and H.-Z. Kou, *Chem. Commun.*, 2014, **50**, 2120−2122.

11 D. Li, S. Parkin, G. Wang, G. T. Yee and S. M. Holmes, *Inorg. Chem*., 2006, **45**, 1951−1959.

12 T. D. Harris and J. R. Long, *Chem. Commun.*, 2007, 1360−1362.

13 (a) E. Fagadar-Cosma, M. C. Mirica, I. Balcu, C. Bucovicean, C. Cretu, I. Armeanu and G. Fagadar-Cosma, *Molecules*, 2009, **14**, 1370−1388; (b) L. Wang, Y. She, R. Zhong, H. Ji, Y, Zhang and X. Song, *Org. Process Res. Dev.*,2006, **20**, 757−761.

14 N. Datta-Gupta, J. C. Fanning and L. L. Dickens, *J. Coord Chem.*, 1976, **5**, 201−207.

15 E. A. Boudreaux and L. N. Mulay, *Theory and Application of Molecular Paramagnetism*, John Wiley & Sons, New York, 1976, pp. 491−494.

16 Bruker; *SMART*, *SAINT* and *XPREP*: Area Detector Control and Data Integration and Reduction Software, Bruker Analytical Xray Instruments Inc., Madison, Wisconsin, USA, 2012.

17 G. M. Sheldrick, *SADABS*: Empirical Absorption and Correction Software, University of Göttingen, Göttingen, Germany, 2012.

18 G. M. Sheldrick, *SHELXS-2014 and SHELXL-2014,* Program for X-ray Crystal Structure Determination, Göttingen University: Göttingen, Germany, 2014.

19 Platon Program: A. L. Spek, *Acta Cryst. Sect. A*., 1990, **46**, 194−201.

20 (a) H. Miyasaka, H. Ieda, N. Matsumoto, K. Sugiura and M. Yamashita, *Inorg. Chem*., 2003, **42**, 3509−3515; (b) H. J. Choi, J. J. Sokol and J. R. Long, *Inorg. Chem*., 2004, **43**, 1606−1608; (c) H. Miyasaka, H. Okawa, A. Miyazaki and T. Enoki, *Inorg. Chem*., 1998, **37**, 4878−4883.

21 O. Kahn, *Molecule Magnetism*, VCH: Weinhem, Germany, 1993.

22 (a) S. M. J. Aubin, Z. Sun, L. Pardi, J. Krzystek, K. Folting, L. C. Brunel, A. L. Rheingold, G. Christou and D. N. Hendrickson, *Inorg. Chem.*, 1999, **38**, 5329−5340; (b) K. S. Cole and R. H. Cole, *J. Chem. Phys.*, 1941, **9**, 341−351; (c) N. Ishii, Y. Okamura, S. Chiba, T. Nogami and T. Ishida, *J. Am. Chem. Soc.*, 2008, **130**, 24−25.

23 (a) H. Miyasaka, N. Matsumoto, H. Okawa, N. Re, E. Gallo and C. Floriani, *J. Am. Chem. Soc.*, 1996, **118**, 981−994; (b) M. Ferbinteanu, H. Miyasaka, W. Wernsdorfer, K. Nakata, K. Sugiura, M. Yamashita, C. Coulon and R. Clérac, *J. Am. Chem. Soc.*, 2005, **127**, 3090−3099; (c) Z.-H. Ni, L.-F. Zhang, V. Tangoulis, W. Wernsdorfer, A.-L. Cui, O. Sato and H.-Z. Kou, *Inorg. Chem.*, 2007, **46**, 6029−6037.

24 (a) H.-R. Wen, C.-F. Wang, Y.-Z. Li, J.-L. Zuo, Y. Song and X.-Z. You, *Inorg. Chem.*, 2006, **45**, 7032−7034; (b) H. Miyasaka, H. Okawa, A. Miyazaki and T. Enoki, *Inorg. Chem.*, 1998, **37**,

4878−4883; (c) W.-W. Ni, Z.-H. Ni, A.-L. Cui, X. Liang and H.-Z. Kou, *Inorg. Chem.*, 2007, **46**, 22−33.
25 (a) H. J. Choi, J. J. Sokol and J. R. Long, *Inorg. Chem.,* 2004, **43**, 1606−1608; (b) D. Zhang, H. Wang, Y. Chen, Z.-H. Ni, L. Tian and J. Jiang, *Inorg. Chem.*, 2009, **48**, 11215−11225.

**Table of Contents Entry**

Three novel cyanide-bridged metalloporphyrinate complexes were synthesized and characterized, and their magnetic properties have been also systematically investigated.